

# Controlling Affinity Binding with Peptide-Functionalized Poly(ethylene glycol) Hydrogels

By Chien-Chi Lin and Kristi S. Anseth\*

Poly(ethylene glycol) (PEG) hydrogels functionalized with peptide moieties have been widely used in regenerative medicine applications. While many studies have suggested the importance of affinity binding within PEG hydrogels, the relationships between the structures of the peptide motifs and their binding to protein therapeutics remain largely unexplored, especially in the recently developed thiol-acrylate photopolymerization systems. Herein, Förster resonance energy transfer (FRET) and thiol-acrylate photopolymerizations are employed to investigate how the architectures of affinity peptides in crosslinked hydrogels affect their binding to diffusible proteins. The binding between diffusible streptavidin and biotinylated peptide immobilized to PEG hydrogel network was used as a model system to reveal the interplay between affinity binding and peptide sequences/architectures. In addition, peptides with different structures are designed to enhance affinity binding within PEG hydrogels and to provide tunable affinity-based controlled delivery of basic fibroblast growth factor (bFGF). This study demonstrates the importance of affinity binding in controlling the availability of hydrogel-encapsulated proteins and provides strategies for enhancing affinity binding of protein therapeutics to bound peptide moieties in thiol-acrylate photopolymerized PEG hydrogels. The results presented herein should be useful to the design and fabrication of hydrogels that retain and exhibit sustained release of growth factors for promoting tissue regeneration.

## 1. Introduction

Poly(ethylene glycol) (PEG) hydrogels are routinely co-polymerized with functional motifs to interact with co-encapsulated cells or growth factors to render the otherwise inert PEG hydrogels bioactive.<sup>[1–6]</sup> For example, cell surface integrin receptor binding peptide sequences, such as Arg-Gly-Asp (or RGD), have been functionalized and copolymerized with PEG-diacrylates (PEG-DAs) to form hydrogels that control/promote cell adhesion and survival.<sup>[1–3]</sup> In the case of controlled protein delivery, several release mechanisms have been proposed to alter the release profiles of therapeutically-relevant proteins, such as growth

factors, from permissible hydrogels. For example, Hubbell and coworkers developed a delivery system where vascular endothelial growth factor (VEGF) was tethered in hydrogels through degradable linkers.<sup>[4,7]</sup> The release rate of the tethered VEGF was dictated by the rate of linker degradation. Although intelligent, this approach requires permanent modification of growth factors that may not be desirable due to the potentially decreased protein bioactivity after structural modification and an enhanced immunogenicity once these modified proteins are released in vivo.

Reversible affinity binding mechanisms, on the other hand, are considered an alternative and effective way of tuning the availability of growth factors in hydrophilic hydrogels without the need to chemically modify valuable protein therapeutics.<sup>[8–13]</sup> Although several affinity matrix systems have been developed so far, most of them involve the use of heparin, a highly sulfated glycosaminoglycan (GAG) that exhibits nonspecific affinity to a variety of growth factors through electrostatic interactions.<sup>[8–10,12]</sup> Further, heparin itself is a highly heterogeneous

large biomacromolecules that may negatively affect the polymerization kinetics. As an alternate, short peptide sequences mimicking the binding of heparin to growth factors have recently been suggested for growth factor binding and release.<sup>[14,15]</sup> For example, Maynard and Hubbell identified a sulfated tetrapeptide that binds to VEGF and suggested its role on fabricating peptide-functionalized biomaterials for VEGF sequestering.<sup>[14]</sup> Further, Willerth et al. utilized phage display screening technique to identify peptide sequences that specifically bind to and subsequently release nerve growth factor (NGF) from fibrin matrices.<sup>[15]</sup> Although this approach eliminates the use of heparin, only limited sustained release of NGF was obtained, suggesting an opportunity for improvements. Furthermore, fibrin-based gels are difficult to manipulate and rapidly degrade in vivo.

Although prior studies have demonstrated the efficacy of affinity binding within hydrogels and obtained a sustained release effect from the “affinity hydrogels”, the relationship between the molecular structure of the functional motifs and affinity binding events remains largely unexplored, especially in peptide functionalized biomaterials. We aimed to design affinity PEG

[\*] Prof. K. S. Anseth, Dr. C.-C. Lin  
Department of Chemical and Biological Engineering  
Howard Hughes Medical Institute  
University of Colorado  
424 UCB, Boulder, Colorado 80309 (USA)  
E-mail: kristi.anseth@colorado.edu

DOI: 10.1002/adfm.200900107

hydrogels capable of tuning the binding and the release of protein therapeutics with the goal of controlling tissue regeneration. In this context, two strategies were utilized to incorporate affinity peptides within PEG hydrogels, including a thiol-acrylate photopolymerization and a semi-interpenetrating network (semi-IPN) entrapping linear affinity peptide within a crosslinked PEG gel. To incorporate peptides within covalently crosslinked gel network, a common approach is to functionalize peptides, on their N-termini, with acryloyl-PEG-NHS (*N*-hydroxysuccinimide) via amine-NHS reaction, followed by radical co-polymerization with PEGDA via chain-growth polymerization mechanism.<sup>[1]</sup> Alternatively, Michael type conjugation reactions can be used to immobilize cysteine-containing peptides in PEG hydrogels through a step-growth polymerization mechanism.<sup>[4]</sup> However, the Michael type addition reaction generally requires careful tuning of the thiol-acrylate ratio to allow gelation, and gel formation can be relatively slow compared to radical-mediated photopolymerizations. Very recently, thiol-acrylate photopolymerizations have emerged as a facile and efficient means of incorporating cysteine-containing peptides within crosslinked hydrogels without the need to chemically modify functional peptide motifs.<sup>[16,17]</sup> Furthermore, it allows for rapidly incorporating peptides at relatively low quantities and yields networks that are useful in directing encapsulated cell fate and controlled release of biomolecules. While previous works have characterized and utilized thiol-acrylate photopolymerization to immobilized short peptide sequences in PEG hydrogels, the use of this polymerization scheme to explore the relationships of peptide architecture and its affinity binding to protein therapeutics have not been proposed. On the other hand, semi-IPN hydrogels containing crosslinked network and stimuli-responsive linear polymer chains have been designed to release biomolecules in response to pH or temperature changes.<sup>[18]</sup> This type of network, however, has not been used in conjunction with affinity binding mechanisms for controlled delivery applications.

Herein, we synthesize peptide functionalized PEG gels using a thiol-acrylate photopolymerization reaction<sup>[16,17]</sup> and employ Förster resonance energy transfer (FRET) to investigate directly how the evolving gel structure and molecular architecture of the affinity peptides affect their binding with diffusible proteins. The binding between biotinylated peptide and streptavidin was used as a model system to reveal the interplay between affinity binding and gel-bound peptide architectures. In addition, we design affinity peptides with different sequences/structures to enhance affinity binding within PEG hydrogels and to provide tunable affinity-based controlled delivery of basic fibroblast growth factor (bFGF).

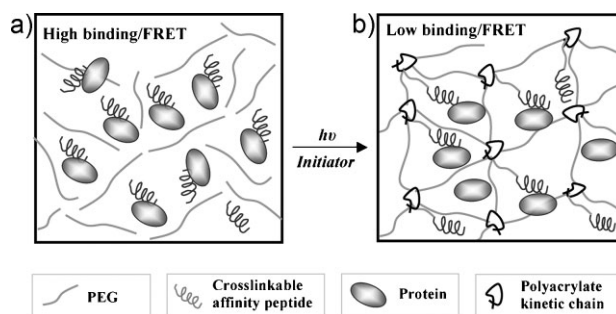
## 2. Results and Discussion

### 2.1. Design of Peptides for Affinity Binding and FRET Measurements

To exploit affinity binding for controlling therapeutic protein delivery from photopolymerized PEG hydrogels, we first examined whether the crosslinking process affects the affinity binding between crosslinkable affinity peptides and diffusible proteins. In addition, we developed a highly versatile hydrogel-

based delivery system incorporating different affinity peptide architectures for sustained growth factor delivery. In situ photopolymerization not only allows for facile incorporation of biomolecules (either crosslinkable or diffusible) during hydrogel fabrication, but also permits simultaneous cell encapsulation for regenerative medicine applications. Prior efforts on controlled protein delivery from affinity hydrogels have revealed disagreements between theoretical predictions and experimental release results.<sup>[11]</sup> We hypothesized that affinity binding between the bound ligand and diffusible protein is negatively affected by the crosslinking process and gel formation, leading to decreased ligand accessibility (Scheme 1). To reveal the relationship between affinity binding and gel formation, we designed affinity binding experiments based on FRET. Specifically, the binding between a photo-crosslinkable biotin and diffusible streptavidin (both were fluorescently labeled) was studied in the presence of PEGDA macromers before, during, and after hydrogel photo-crosslinking. FRET has been used to examine the binding between cell surface integrin receptors and immobilized RGD peptides in alginate hydrogels<sup>[19,20]</sup> as well as the affinity binding between two soluble proteins within polyacrylamide hydrogels.<sup>[21]</sup> However, it has not been used to study the binding between gel-bound affinity peptides and soluble proteins, nor has it been used to reveal the importance of peptide architectures within material microenvironments on affinity binding events. The uniqueness of photopolymerization to control the polymerization kinetics temporally further allows us to monitor the affinity binding events at any instant during gel formation (i.e., as the crosslinking density evolves).

To this end, we have synthesized tri-functional peptides containing i) C-terminal cysteine for peptide immobilization through the thiol-acrylate photopolymerization,<sup>[16,17]</sup> ii) N-terminal biotin-label for streptavidin-biotin binding, and iii) FITC-label near biotin for FRET measurement. This polymerizable peptide, Biotin-GK(FITC)GGC (Biotin-FITC-G2), was used as an FRET donor, while the diffusible AlexaFluor 555-labeled streptavidin (AF555-SA) was used as an FRET acceptor (Table 1). The presence of cysteine residue on the biotinylated peptide permits efficient peptide incorporation and



**Scheme 1.** Affinity binding between peptide ligand and diffusible protein in PEGDA macromer solution (a) and in PEG hydrogel after photopolymerization (b). The binding is initially high when both the protein and affinity peptide are freely diffusible. However, once the PEGDA macromers are crosslinked into gels, the steric hindrance of polyacrylate kinetic chains and hydrophilic PEG chains decreases the binding of soluble protein to the immobilized affinity peptides.

**Table 1.** Affinity binding pairs used in FRET experiments.

Protein	Affinity peptide ligand	Designed peptide sequence [a]
AlexaFluor 555 conjugated Streptavidin (AF555-SA)	Biotin-FITC-G2	Biotin-GK(FITC)GGC
	Biotin-FITC-G7	Biotin-GK(FITC)GGGGGGGC
	Biotin-FITC-G12	Biotin-GK(FITC)GGGGGGGGGGGGC
AlexaFluor 555 conjugated bFGF (AF555-bFGF)	Mono-bFGF-bp [b]	CGGK(FITC)GKRTGQYKL
	Multi-bFGF-bp	Linear-GGK(FITC)GKRTGQYKL

[a] Cysteine was added to the peptide sequence for peptide incorporation in PEGDA hydrogels through thiol-acrylate photopolymerization. [b] Multivalent bFGF binding peptide (multi-bFGF-bp) was synthesized from monovalent bFGF binding peptide (mono-bFGF-bp).

immobilization within PEGDA hydrogels according to the mixed-mode, thiol-acrylate photopolymerization mechanism,<sup>[16,17]</sup> while the presence of biotin and FITC allow for affinity binding to AF555-SA and FRET measurement, respectively.

## 2.2. Affinity Binding During the Evolution of the Hydrogel Network

We first examined FRET, an indication of affinity binding, of the synthesized Biotin-FITC-G2 peptide and AF555-SA at constant donor concentration (2000 nM Biotin-FITC-G2 peptide) in phosphate buffered solution (PBS). As shown in Figure 1, increasing FRET as a function of AF555-SA represents increases in biotin-streptavidin binding. We next examined the affinity binding events in PEGDA (10 kDa, 10 wt %) macromer solutions before photopolymerization and in PEG hydrogels after photopolymerization (Fig. 2A). It was found that normalized FRET, in PEGDA solution increases as increasing acceptor (AF555-SA) concentrations, indicating increased biotin-streptavidin binding. The results of increasing FRET shown in Figure 1 and 2A are not surprising as the occurrence of FRET are an indication of donor-acceptor affinity binding. What is interesting is that when the same macromer solutions were photopolymerized to form PEG

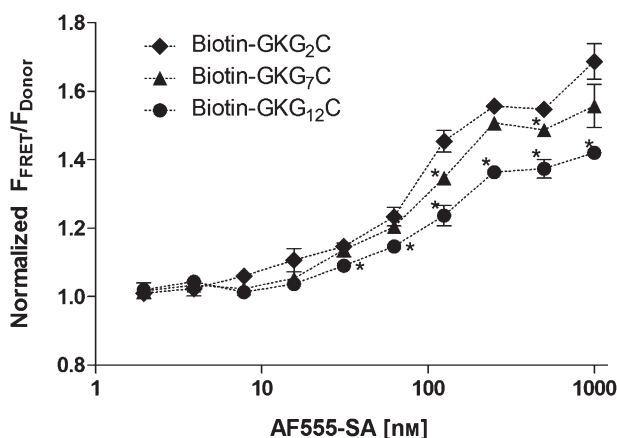


**Figure 1.** FRET of AlexaFluor555-SA and biotin-peptide (2000 nM) with different spacer lengths in PBS. FRET was expressed as ratios of the fluorescence in the FRET filter or  $F_{\text{FRET}}$  (Ex: 485 nm, Em: 590 nm) and the fluorescence in the donor filter or  $F_{\text{donor}}$  (Ex: 485 nm, Em: 535 nm) without further calibration. (Asterisks designate statistical significant as per students' *t*-test compared to Biotin-GKG<sub>2</sub>C group;  $N = 4$ , mean  $\pm$  SEM;  $p < 0.05$ ).

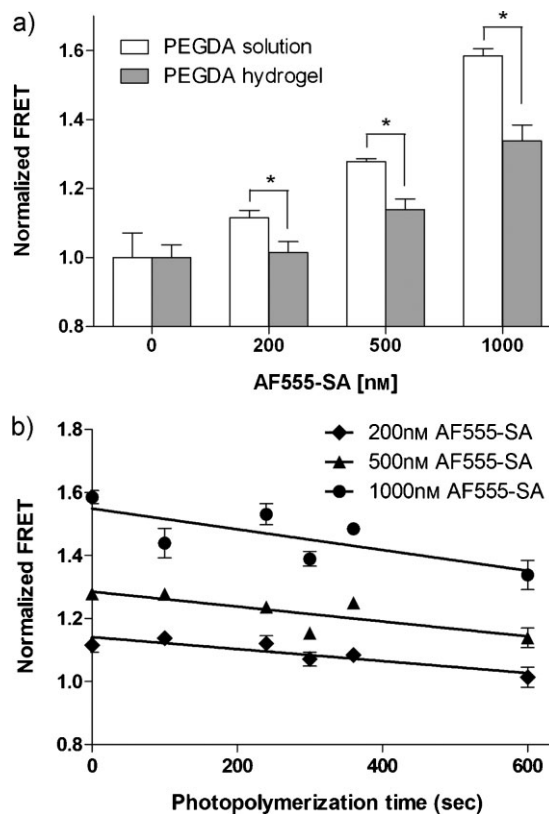


**Figure 2.** a) Normalized FRET as functions of acceptor (AF555-SA) concentration at constant donor (Biotin-GK(FITC)GGC) concentration (2000 nM) in PEGDA solutions or hydrogels (asterisks designate statistical significant as per students' *t*-test performed between indicated groups;  $N = 4$ , mean  $\pm$  SEM;  $p < 0.05$ ). Noted that the normalized FRET was calibrated results based on equations provided in the Supporting Information. b) Normalized FRET as functions of photopolymerization time at constant donor concentration (2000 nM). Straight lines were the results of linear regression and all exhibit negative slopes, indicating decline in the normalized FRET as a function of photopolymerization time. ( $N = 4$ , mean  $\pm$  SEM) see Table 2 for statistical analysis of the linear regression.

hydrogels, the degree of FRET decreases as a function of photopolymerization time (Fig. 2B). Statistical analysis results reveal that all three linear regression best fit curves exhibit negative slopes (Table 2), indicating a declining trend in the normalized FRET (i.e., peptide-protein binding) as a function of photopolymerization time. Further, the fluorescence of FITC and AF555 in PEGDA macromer solutions remains relatively

**Table 2.** Statistical analysis of photopolymerization time-dependent decrease of FRET.

AF555-SA [nM] [a]	Slope of linear regression curve [ $\times 10^{-4}$ ]	<i>p</i> -value [b]
200	$-1.902 \pm 0.4794$	0.017
500	$-2.364 \pm 0.8617$	0.052
1000	$-3.287 \pm 1.418$	0.081

[a] Donor concentration was fixed at 2000 nM. [b] *p*-values represent 95% confidence intervals of the linear regression analysis compared to zero-slope.

constant (see Supporting Information Fig. S1), implying that the decrease in FRET is due to decreased affinity binding, but not due to a decrease in the fluorescence of either fluorophore. We reasoned that once the initially diffusible biotinylated peptide becomes immobilized and non-diffusible during the gelation process, the peptide is embedded within the hydrophilic PEG chains and less accessible for binding (Scheme 1).

### 2.3. Addition of Peptide Spacers to Enhance Affinity Binding

In order to further demonstrate that the decreased FRET (and decreased affinity binding) is indeed due to the limited accessibility of the immobilized ligands to the diffusible proteins, we designed other biotinylated peptides with 7 and 12 glycine spacers, respectively (Biotin-FITC-G7, Biotin-FITC-G12, Table 1). We hypothesized that the added glycine spacers would extend the affinity binding motif (biotin) away from the crosslinking point (C-terminal cysteine) such that steric hindrance due to surrounding PEG molecules would be decreased and an increased affinity binding between the immobilized ligand and diffusible protein would be obtained. As shown in Figure 1, no differences were found in the binding of Biotin-FITC-G2 or Biotin-FITC-G7 to AF555-SA in PBS. However, the binding between Biotin-FITC-G12 to AF555-SA was found to decrease slightly in PBS. We reasoned that the decreased biotin-streptavidin binding for the Biotin-FITC-G12 in PEGDA macromer solution may be due to the shielding of some biotin by the longer peptide tail that limits its binding to streptavidin. However, the benefits of long spacers on affinity binding stand out after the photopolymerization process to crosslink the hydrogel network and protein-binding peptide. As shown in Figure 3, no differences in normalized FRET were found for the biotin-streptavidin binding pairs in PEGDA solution, except for the biotinylated peptide with 12 glycines (Biotin-FITC-G12). Importantly, when the PEGDA macromer solutions containing AF555-SA and biotinylated peptides (Biotin-FITC-G2, Biotin-FITC-G7, or Biotin-FITC-G12) were photopolymerized, we observed increased normalized FRET with increasing length of the glycine spacers. To the best of our knowledge, this is the first example of using FRET measurements to quantify directly affinity binding between free diffusible proteins and peptide ligands bound within a biomaterial environment. Further, this approach allowed us to demonstrate conclusively the critical role of spacing between the peptide tether and the binding motif on affinity binding, and ultimately, protein release from the gel.

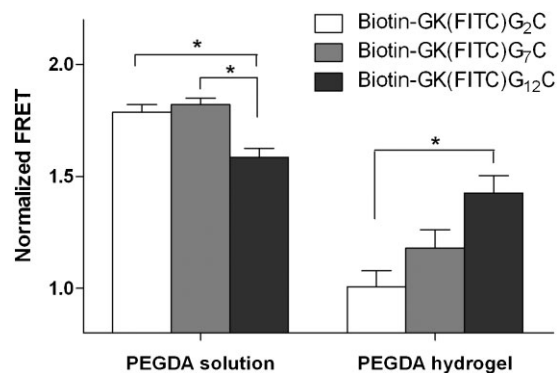


**Figure 3.** Normalized FRET of biotin-streptavidin binding with different spacer length and in different PEG environments (solution or hydrogel) at constant donor (biotinylated peptide; 1000 nM) and acceptor (AF555-SA; 1000 nM) concentrations. (Asterisks designate statistical significance as per students' *t*-test performed between indicated groups; *N* = 4, mean  $\pm$  SEM; *p* < 0.05).

### 2.4. Semi-IPN Affinity Hydrogels for bFGF Sequestering

The incorporation of affinity binding peptides within PEG hydrogels to control protein-peptide interactions can be achieved via simple thiol-acrylate photopolymerization as described above. On the other hand, affinity peptides can be conjugated on linear polymer chains to yield multivalent ligands with increased binding affinity or bioactivity. Many studies have revealed the beneficiary effects of multivalent protein-receptor binding on enhancing receptor-mediated signaling events.<sup>[22,23]</sup> However, utilizing multivalent protein-peptide binding to control affinity-based protein release has not been proposed. To this end, we synthesized monovalent, as well as multivalent, affinity peptides to control protein-peptide interactions within and protein release from photopolymerized PEG hydrogels. Specifically, bFGF was selected, due to its importance in tissue engineering and regenerative medicine applications, as a model protein to demonstrate the concept of affinity-based controlled release. Previous research has been suggested that the peptide sequence (KRTGQYKL), originally derived from bFGF (119–126), interacts with bFGF itself, rather than binding to the bFGF receptor.<sup>[24–27]</sup> Furthermore, the crystal structure and site-directed mutagenesis results reveal that the amino acid residues in KRTGQYKL do not contribute to the binding between bFGF and bFGF-R.<sup>[28]</sup> This peptide sequence has also been conjugated to liposome and bovine serum albumin (BSA) for binding to bFGF and to increase bFGF-R binding.<sup>[25,27]</sup>

To verify the binding of KRTGQYKL peptide to bFGF in 3D PEG hydrogels, we synthesized a tri-functional peptide analog (Table 1) that contains i) bFGF binding motif (KRTGQYKL), ii) N-terminal cysteine for thiol-acrylate polymerization, and iii) FITC labeling for FRET measurement. We examined the monovalent affinity binding between AF555-labeled bFGF and monovalent bFGF-binding peptide (mono-bFGF-bp) in PEGDA (10 kDa) solutions and hydrogels, respectively. Figure 4A shows that, similar to Figure 2, the binding of bFGF to peptide ligands increases with increasing bFGF concentrations. However, the degree of binding decreases

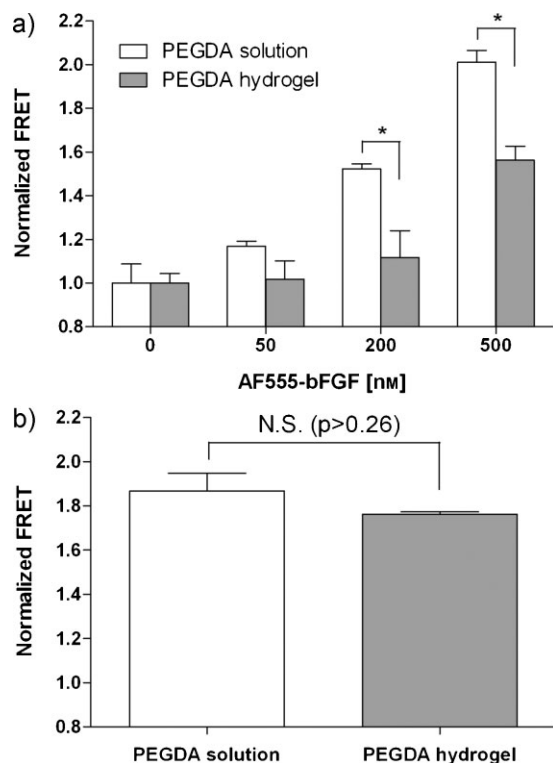


**Figure 4.** a) Comparison of normalized FRET of bFGF—monomeric KRTGQYKL binding in PEG solution or reacted into PEG hydrogels as a function of acceptor (AF555-bFGF) concentration (donor concentration: 500 nm). (Asterisks designate statistical significance as per students' *t*-test performed between indicated groups;  $N = 3$ , mean  $\pm$  SEM;  $p < 0.05$ ). b) Normalized FRET of bFGF-multivalent KRTGQYKL binding in PEG solution or entrapped in PEG hydrogels (donor concentration equivalent to 500 nm monomeric KRTGQYKL; acceptor concentration: 500 nm). No statistical difference was found between PEG solution and hydrogel (student's *t*-test,  $N = 3$ , mean  $\pm$  SEM;  $p > 0.26$ ).

after photo-crosslinking of PEGDA and bFGF-binding peptide to form affinity PEG hydrogels (Fig. 4A). This evidence reveals the wide-spread phenomenon of how the gel microenvironment can negatively affect protein binding to matrix-bound peptides. To further enhance the affinity protein-peptide binding within photopolymerized hydrogels, we synthesized multivalent bFGF binding peptide (multi-bFGF-bp) on poly(acrylic acid) polymer chains according to an established conjugation scheme<sup>[23]</sup> (Supporting Information Fig. S3). The resulting linear multivalent peptides were then mixed with a PEGDA macromer solution and photopolymerized to form a semi-IPN containing crosslinked PEG hydrogel and linear multivalent bFGF-binding peptides. The semi-IPN hydrogels possess two major advantages: i) since the peptide ligands are pre-conjugated to a linear polymer chain, no further crosslinking process occurs between the linear multivalent peptides and PEGDA macromer during photopolymerization. This may decrease steric hindrance due to surrounding PEG molecules that limits the accessibility of the affinity binding peptide to bFGF; and ii) enhanced bFGF binding may be obtained due to the presence of multivalent affinity binding peptides. Taken together, this approach may result in a better binding for controlling bFGF availability within or release

from PEG hydrogels. We confirmed the enhanced affinity binding using FRET measurement. As shown in Figure 4B, no statistical differences in normalized FRET were found between the bFGF-peptide affinity binding in PEGDA solutions and in crosslinked hydrogels, indicating a similar degree of binding between bFGF and the linear multivalent peptides.

To further demonstrate the binding affinity between bFGF and network immobilized KRTGQYKL, we performed bFGF loading/absorption studies by incubating PEG hydrogels functionalized with i) affinity peptide KRTGQYKL or ii) scramble peptide KGRYQKTL in concentrated bFGF solutions and quantifying the amount of bFGF absorbed in gels. As shown in Figure 5a, the amount of bFGF absorbed into PEG hydrogels increases dose-dependently at increasing affinity peptide (KRTGQYKL) concentrations. However, the use of the scrambled peptide (KGRYQKTL) does not affect the amount of bFGF loaded into the peptide-functionalized PEG hydrogels. Furthermore, the use of multivalent KRTGQYKL peptide further increases the absorption of bFGF within gels at a lower equivalent peptide concentration ( $28.3 \pm 0.68$  and  $27.3 \pm 0.44$  ng mg<sup>-1</sup> gel for 2.2  $\mu$ M multivalent and 4.4  $\mu$ M monovalent peptide, respectively).

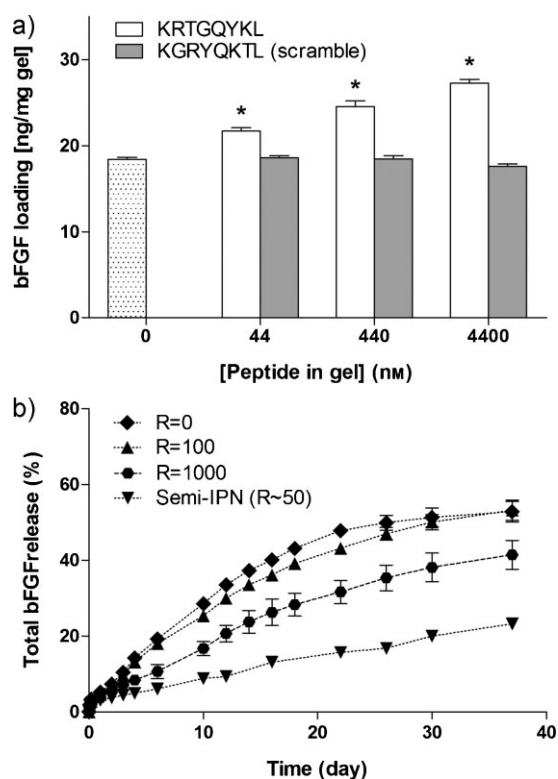


**Figure 5.** a) bFGF loading/absorption into 10 wt % PEG-10 kDa hydrogels (dotted bar) or PEG gels functionalized with KRTGQYKL (white bars) or scrambled KGRYQKTL peptide (gray bars). Asterisks designate statistical significance compared to unmodified PEG hydrogels as per students' *t*-test ( $N = 3$ , Mean  $\pm$  SEM;  $p < 0.05$ ). b) Sustained release of bFGF from affinity peptide (KRTGQYKL) functionalized PEG hydrogels (10 kDa, 10 wt %). bFGF was encapsulated ( $750$  ng gel<sup>-1</sup>) in PEG hydrogels in situ during photopolymerization with different affinity peptide concentrations and architecture.  $R = 0$  ( $\diamond$ ); 100 ( $\triangle$ ); 1000 ( $\circ$ ); semi-IPN,  $R = 50$  ( $\times$ ). ( $N = 3$ , mean  $\pm$  SEM).

Collectively, the FRET measurements, as well as the bFGF absorption experiments, demonstrate that the peptide KRTGQYKL is an affinity binder for bFGF and interacts with it in a dose-dependent manner.

## 2.5. Sustained Release of bFGF from Affinity Hydrogels

From the perspective of controlled release, the direct impact of increasing affinity binding between growth factors and affinity peptides is an extended growth factor release profile that could enhance growth factor induced tissue regeneration. To verify that increasing affinity binding indeed results in sustained growth factor release and an enhanced therapeutic efficacy, we performed *in vitro* bFGF release experiments from inert or affinity PEG hydrogels. Monomeric bFGF binding peptide was incorporated within PEGDA hydrogels through the mixed-mode thiol-acrylate photopolymerization. As shown in Figure 5b, total release of bFGF from PEGDA hydrogels was retarded as increasing ligand-to-protein ratio. However, it can be seen that the use of ligand-to-protein ratio at  $R=100$  only slightly decreased the release of bFGF and a significant sustained release effect was observed at high ligand-to-protein ratio ( $R=1000$ ). As determined in a prior study, KRTGQYKL peptide binds to bFGF with an equilibrium dissociation constant ( $K_D$ ) of 122 nM,<sup>[25]</sup> indicating that this peptide is a high affinity binder. Based on this  $K_D$ , we calculated (see Supporting Information for detail) the equilibrium binding of bFGF to KRTGQYKL in solution and revealed that an  $R$  value of 100 should yield over 97% of protein bound, in an equilibrium condition, to affinity peptide ligand (Fig. S3 of Supporting Information) and should provide significant sustained release effect when incorporated within hydrogel. However, we only observed a slight decrease in bFGF release (compared to PEG-only hydrogels) when monomeric bFGF binding peptide (CGKRTGQYKL) at  $R=100$  was incorporated covalently within PEG hydrogels, indicating that the initially high degree of equilibrium ligand-protein binding in solution was largely decreased after the peptide ligands were covalently immobilized within the hydrogel network (Fig. 4a).

To overcome the limited sustained release effect provided by direct co-polymerization of the affinity peptide ligand within the PEG hydrogel network, we fabricated semi-IPN hydrogels containing a linear multivalent bFGF-binding peptide entrapped with a crosslinked PEG gel. As shown in Figure 5b, a significant sustained bFGF release was observed when the semi-IPN affinity hydrogels were used. Importantly, this sustained release effect was obtained at a much lower ligand-to-protein ratio ( $R=50$ ), indicating the superior affinity binding and sustained release effects provided by multivalent linear affinity peptide. Furthermore, the released bFGF remained bioactive, as it successfully induced the *in vitro* differentiation of PC12 pheochromocytoma cell line in a gel-cell transwell culture system (Supporting Information, Fig. S5).

## 3. Conclusions

In conclusion, we developed a versatile affinity PEG hydrogel system based on reversible protein-peptide binding to control the affinity binding and sustained release of protein therapeutics.

Taking advantages of FRET phenomena and temporal-control over photopolymerization kinetics, we reveal the effects of peptide architectures and conjugation methods on protein-peptide affinity binding and have devised strategies to enhance the affinity binding within crosslinked PEG hydrogels. Furthermore, we demonstrate that the degree of protein-ligand affinity binding decreases as a function of hydrogel crosslinking and formation. We also illustrate how affinity binding in and the subsequent release of growth factor from PEG hydrogels can be manipulated through controlling any of the following parameters: i) architecture of the affinity peptide, ii) valency of the affinity peptides, and iii) the ratio of protein-to-ligand. The versatility of this affinity hydrogel platform stems from the facile *in situ* hydrogel fabrication and affinity peptide incorporation. In the context of controlled growth factor delivery, the manipulation of affinity binding within permissible PEG hydrogels can directly impact the bioavailability of the growth factors and the fate of growth factor induced tissue regeneration. Although not shown in this contribution, the ability to retain growth factors within PEG hydrogels through specific peptide-protein affinity binding should prove useful in directing cell fate and secretory functions in 3D hydrogel environment. The affinity hydrogel system for growth factor delivery (or retention) developed herein can be readily adapted to a variety of regenerative medicine applications, such as growth factor mediated wound healing and controlled stem cell differentiation.

## 4. Experimental

**Materials:** Amino acids for solid phase peptide synthesis were purchased from Anaspec (Anaspec Inc. CA, USA). AlexaFluor 555 conjugated streptavidin and protein conjugation kit (for bFGF conjugation) were obtained from Invitrogen (Invitrogen Inc., CA, USA). FITC and EMCH crosslinker were obtained from PIERCE (Thermo Fisher Scientific Inc., IL, USA). Recombinant human bFGF and bFGF ELISA development kit were purchased from Peprotech (PeproTech Inc., NJ, USA). All chemicals were obtained from Sigma-Aldrich (St. Louis, MO, USA) unless otherwise noted.

**Poly(ethylene glycol) Diacrylate Synthesis:** PEGDA was synthesized as previously described [11,13] by reacting PEG macromer with an average molecular weight of 10 000 Da (Sigma-Aldrich) with acryloyl chloride (Sigma-Aldrich) in the presence of triethylamine (TEA). Briefly, measured amount of PEG was reacted with 8 mol excess of acryloyl chloride for overnight at room temperature in dark. The acrylated PEG was filtered through alumina to remove the TEA-HCl complex. Toluene was then removed from the product mixture under vacuum using a Rotovap. To obtain pure PEGDA, the crude product was dissolved in dichloromethane and precipitated in chilled diethyl ether. The purified PEGDA was then filtered and dried under vacuum at room temperature. A degree of acrylation above 95% was determined using <sup>1</sup>H NMR.

**Peptide Synthesis and Modification:** All peptides were synthesized on a solid phase peptide synthesizer (Applied Biosystems, Model 433A). After solid phase peptide synthesis, resin bound, and side-chain protected peptides were biotinylated by conjugating activated carboxyl-biotin to the N-terminal primary amines. The completion of biotinylation was determined by Ninhydrin assay. Lys(Mtt) (Anaspec) was incorporated in the peptide sequence for site-specific FITC labeling. After selective removal of the Mtt group by treating the protected and resin-bound peptides with 1% trifluoroacetic acid (TFA), fluorescein isothiocyanate (FITC) was reacted overnight to the primary amine of the selectively de-protected lysine. After biotinylation and FITC-labeling, the peptide was fully de-protected and cleaved from the resin using a cleavage cocktail containing

5 wt% phenol in 95% TFA, 2.5% triisopropylsilane (TIPS), and 2.5% water. Cleaved peptides were purified by reverse-phase HPLC and characterized by MALDI-TOF mass spectroscopy. Monovalent and FITC-labeled bFGF-binding peptide, CCGK(FITC)GKRTGQYKL, was synthesized using procedures similar to the process described above.

**Multivalent bFGF-Binding Peptide Synthesis:** Multivalent bFGF-binding peptide was synthesized from monovalent bFGF-bp according to a published reaction scheme (Supporting Information) [23]. Briefly, carboxylic acids of linear poly(acrylic acid) (or Poly(AAc), MW: 1 000 000 Da) were activated using EDC/NHS chemistry. Carboxylate-activated Poly(AAc) chains were then reacted with the amine group of a bi-functional crosslinker, EMCH (PIERCE), creating maleimide-bearing, thiol-reactive Poly(AAc) chains. Finally, CCGK(FITC)GKRTGQYKL peptide was reacted with the thiol-reactive Poly(AAc) chains through a thiol-maleimide reaction. The activated and peptide-conjugated Poly(AAc) chains were purified on a microcentrifugal device with a 50 kDa molecular weight cutoff. The appearance and disappearance of maleimide groups on Poly(AAc) chains (monitored with UV/Vis spectroscopy) were used as an indication of EMCH and peptide conjugation, respectively (Fig. S2 of Supporting Information).

**PEG Hydrogel Synthesis:** The fabrication of PEG hydrogels with or without peptide was accomplished via photopolymerization. Briefly, 10 wt% PEGDA solutions containing desired concentrations of peptide ligand, protein, and 0.025 wt% photoinitiator (Irgacure-2959) were incubated for 45 min, followed by 10 min of photopolymerization (365 nm, 8.5 mW cm<sup>-2</sup>) under ambient conditions.

**FRET Measurement and Calculation:** FITC-labeled peptides were used as an FRET donor while AlexaFluor 555-labeled streptavidin (AF555-SA, obtained from Invitrogen) or bFGF (AF555-bFGF, labeled with AF555 labeling kit, Invitrogen) was used as an FRET acceptor. Samples composed of acceptor-only, donor-only, and acceptor-donor in 10 wt% PEGDA solutions were mixed in a black 96-well plate for 45 min prior to FRET measurement. The fluorescence at three filter-sets (acceptor filter, donor filter, and FRET filter) was measured in a microplate reader (Perkin Elmer Wallac Victor 2, 1420 Multilabel Counter). The obtained fluorescence was calibrated using specified bleed through with donor and acceptor only corrections. The FRET signals of the donor-only samples were used to normalized FRET signals of donor-acceptor samples and expressed as "Normalized FRET" (see Supporting Information for details) For time-dependent FRET measurements, the 96-well plate containing FRET samples was removed from UV light source at pre-determined time interval and immediately placed in the microplate reader for FRET measurements.

**bFGF Loading/Absorption in PEG Hydrogels:** bFGF loading/absorption in peptide-functionalized PEG hydrogels was accomplished by incubating pre-swelled PEG hydrogels functionalized with different amounts of the affinity peptide KRTGQYKL or scramble peptide KGRYQKTL in 0.8 mL of recombinant bFGF solution (1 µg mL<sup>-1</sup>). After incubating for 3 days, the concentration of bFGF in the supernatant was quantified via a bFGF ELISA (Peprotech), and the difference between the initial amount and the remaining amount of bFGF in the supernatants was calculated to determine the bFGF absorption in the gel. The final bFGF loading in the gels was normalized to the measured gel swollen weight.

**In Vitro bFGF Release:** Human bFGF (Peprotech) was incubated with affinity peptide in 10 wt% PEGDA (MW: 10 kDa) solution for 45 min prior to photopolymerization. After gelation, the gels (thickness = 1 mm) were punch out using a 5 mm diameter biopsy punch. The concentration of bFGF in each gel was 750 ng gel<sup>-1</sup>. For in vitro release, bFGF-loaded gels were placed in 1 mL of PC12 cell differentiation medium composed of RPMI-1640 (Gibco), 1% horse serum, 1% penicillin-streptomycin, and 0.5 µg mL<sup>-1</sup> fungizone. At pre-determined time interval, gels were transferred to fresh media and the old media containing released bFGF were collected and stored at -80 °C until assay. The concentrations of released bFGF were quantified using human bFGF ELISA kit (Peprotech).

## Acknowledgements

The authors thank Sarah Trexler for her technical assistance on solution FRET measurements. This work was supported by NIH (5R01DK076084) and the Howard Hughes Medical Institute. Supporting Information is available online from Wiley InterScience or from the author.

Received: January 21, 2009

Revised: February 15, 2009

Published online: May 14, 2009

- [1] D. L. Hern, J. A. Hubbell, *J. Biomed. Mater. Res.* **1998**, *39*, 266.
- [2] B. K. Mann, A. S. Gobin, A. T. Tsai, R. H. Schmedlen, J. L. West, *Biomaterials* **2001**, *22*, 3045.
- [3] J. A. Burdick, K. S. Anseth, *Biomaterials* **2002**, *23*, 4315.
- [4] A. H. Zisch, M. P. Lutolf, M. Ehrbar, G. P. Raeber, S. C. Rizzi, N. Davies, H. Schmokel, D. Bezuidenhout, V. Djonov, P. Zilla, J. A. Hubbell, *FASEB J.* **2003**, *17*, 2260.
- [5] S. A. DeLong, J. J. Moon, J. L. West, *Biomaterials* **2005**, *26*, 3227.
- [6] C. C. Lin, K. S. Anseth, *Pharm. Res.* **2009**, *26*, 631.
- [7] M. Ehrbar, V. G. Djonov, C. Schnell, S. A. Tschanz, G. Martiny-Baron, U. Schenk, J. Wood, P. H. Burri, J. A. Hubbell, A. H. Zisch, *Circ. Res.* **2004**, *94*, 1124.
- [8] S. E. Sakiyama-Elbert, J. A. Hubbell, *J. Controlled Release* **2000**, *69*, 149.
- [9] S. E. Sakiyama-Elbert, J. A. Hubbell, *J. Controlled Release* **2000**, *65*, 389.
- [10] G. Tae, M. Scatena, P. S. Stayton, A. S. Hoffman, *J. Biomater. Sci., Polym. Ed.* **2006**, *17*, 187.
- [11] C. C. Lin, A. T. Metters, *J. Biomed. Mater. Res., Part A* **2007**, *83A*, 954.
- [12] D. S. W. Benoit, S. D. Collins, K. S. Anseth, *Adv. Funct. Mater.* **2007**, *17*, 2085.
- [13] C. C. Lin, A. T. Metters, *Biomacromolecules* **2008**, *9*, 789.
- [14] H. D. Maynard, J. A. Hubbell, *Acta Biomater.* **2005**, *1*, 451.
- [15] S. M. Willerth, P. J. Johnson, D. J. Maxwell, S. R. Parsons, M. E. Doukas, S. E. Sakiyama-Elbert, *J. Biomed. Mater. Res., Part A* **2007**, *80A*, 13.
- [16] C. N. Salinas, B. B. Cole, A. M. Kasko, K. S. Anseth, *Tissue Eng.* **2007**, *13*, 1025.
- [17] C. N. Salinas, K. S. Anseth, *Macromolecules* **2008**, *41*, 6019.
- [18] H. K. Ju, S. Y. Kim, Y. M. Lee, *Polymer* **2001**, *42*, 6851.
- [19] H. J. Kong, T. R. Polte, E. Alsberg, D. J. Mooney, *Proc. Natl. Acad. Sci. U. S. A.* **2005**, *102*, 4300.
- [20] H. J. Kong, T. Boonthekul, D. J. Mooney, *Proc. Natl. Acad. Sci. U. S. A.* **2006**, *103*, 18534.
- [21] J. Moorthy, R. Burgess, A. Yethiraj, D. Beebe, *Anal. Chem.* **2007**, *79*, 5322.
- [22] M. C. Cushing, J. T. Liao, M. P. Jaeggli, K. S. Anseth, *Biomaterials* **2007**, *28*, 3378.
- [23] S. T. Wall, K. Saha, R. S. Ashton, K. R. Kam, D. V. Schaffer, K. E. Healy, *Bioconjugate Chem.* **2008**, *19*, 806.
- [24] A. Yayon, D. Aviezer, M. Safran, J. L. Gross, Y. Heldman, S. Cabilly, D. Givol, E. Katchalskikatzir, *Proc. Natl. Acad. Sci. U. S. A.* **1993**, *90*, 10643.
- [25] T. Terada, M. Mizobata, S. Kawakami, Y. Yabe, F. Yamashita, M. Hashida, *J. Drug Targeting* **2006**, *14*, 536.
- [26] L. Kinsella, H. L. Chen, J. A. Smith, P. S. Rudland, D. G. Fernig, *Glycoconjugate J.* **1998**, *15*, 419.
- [27] T. Terada, M. Mizobata, S. Kawakami, F. Yamashita, M. Hashida, *J. Controlled Release* **2007**, *119*, 262.
- [28] B. A. Springer, M. W. Pantoliano, F. A. Barbera, P. L. Gunyuzlu, L. D. Thompson, W. F. Herblin, S. A. Rosenfeld, G. W. Book, *J. Biol. Chem.* **1994**, *269*, 26879.